Preprints of the 23rd IFAC World Congress
Busan, Republic of Korea, August 23-28, 2026

Tracking Stability of Multi-UAVs against Deterministic and Stochastic Disturbances

Feng Yang, * **Qi Mao,** * **Shi Li,** * **Lu Cong,** ** **Yifan Zhang,** *
Jun Chen *

* *School of Electrical and Automation Engineering, Nanjing Normal University, Nanjing, China (e-mail: 21230720@njnu.edu.cn, qmao_eae@nnu.edu.cn).*
** *School of Air Transport and Engineering, Nanhang Jincheng College, Nanjing, China.*

Abstract: In this paper, we investigate the tracking stability of phase-shifted circular reference trajectories in multi-UAV systems subject to deterministic disturbances, stochastic perturbations, and actuator saturation, whereby a trend-driven adaptive annealed-PID tracking strategy is then proposed. Within this framework, a low-pass filtered trend of the error energy for each vehicle regulates a slow outer-loop that adaptively modulates bounded PID gains. Meanwhile, the inner loop ensures continuous control via leaky integration and anti-windup compensation. Drawing upon the polytopic vertex–linear matrix inequality (LMI) framework, we establish input-to-state stability under deterministic disturbances and mean-square boundedness under stochastic perturbations. Numerical simulations demonstrate the effectiveness and robustness of the developed tracking control approach.

Keywords: Multi-UAV, trajectory tracking, stability, gain scheduling, and PID control.

1. INTRODUCTION

Tracking problems in multi-agent systems (MAS) have attracted extensive attention due to their critical role in practical applications such as unmanned aerial vehicle (UAV) trajectory coordination in Su et al. (2023), distributed sensing in Wang et al. (2025), and cooperative transportation in Sun et al. (2023). As network scales grow and task complexity increases, a central challenge lies in designing scalable control laws that guarantee reliable trajectory tracking—particularly for multi-UAV systems, see e.g., Pan et al. (2022)—operating in highly dynamic environments subject to various disturbances, see e.g., Wei et al. (2021).

Among control strategies for multi-UAV systems, consensus is generally categorized into complete consensus and group consensus (De Pasquale et al. (2022)). With the expansion of network scale and advances in distributed optimal control, the research focus has gradually shifted from achieving global consensus across the entire network to establishing cluster consensus within local subgroups under limited communication, and then propagating these local agreements to obtain a network-wide solution (see, e.g., De Pasquale et al. (2022); Guo and Meng (2023)). Different from such neighbor-coupled consensus formulations, this paper considers a synchronized tracking architecture, in which phase-shifted circular reference trajectories are assigned to individual UAVs, and each vehicle tracks its own reference using local feedback. Two major methodological directions have emerged in this context: robust-optimization approaches and adaptive approaches.

Robust-optimization methods aim to design controllers capable of withstanding worst-case disturbances and parametric uncertainties. Techniques such as high-order sliding-mode control fall into this category, though they may suffer from chattering and noise sensitivity Li et al. (2024). Recent advances also integrate uncertainty directly into the optimization layer, as seen in Wasserstein distributionally robust control Hakobyan and Yang (2024), which improves robustness under distributional ambiguity but may increase computational burden. In contrast, adaptive methods adjust the controller structure online to handle uncertainties or time-varying agent dynamics, see e.g., Ahmadian et al. (2024); Tao (2025). For stochastic nonlinear systems, event-triggered Itô-system control with state quantization has also been studied in Sun et al. (2024).

Existing control strategies, though partially adaptive, still depend on predefined parameter ranges or online optimization, which often leads to irregular gain behaviors and high computational burden; moreover, the absence of unified stability guarantees under highly dynamic and stochastic environments further undermines tracking performance. With the evolution of control principles from empirical tuning to analytical design, PID control has emerged as one of the most widely adopted techniques in engineering practice Mao et al. (2023, 2025). This prevalence stems mainly from its structural simplicity, ease of implementation, and low operational cost.

⋆ This research was supported by the Natural Science Foundation of Jiangsu Province of China under Grant BK20250630, in part by the Natural Science Research Project of Jiangsu Higher Education Institutions under Grant 24KJB120009, and in part by the Research Start Fund of Nanjing Normal University under Grant 184080H201B68. *Corresponding author: Qi Mao.*

©2026 the authors. Accepted by IFAC for publication under a Creative Commons Licence CC-BY-NC-ND

Building on the structural simplicity of PID control and the annealing concept in Barzegar et al. (2024), this paper presents a dual-loop PID controller with annealed gains driven by the error trend, which aims to achieve robust tracking of phase-shifted circular reference trajectories in a local multi-UAV system. The main contributions of this paper are summarized as follows. First, an annealing adaptive gain model, driven by the trend of the error energy, is constructed and embedded into an augmented PID control law, providing an intrinsic mechanism for smooth gain adaptation and effective disturbance attenuation. To cope with highly dynamic environments and stochastic disturbances, a fast–slow dual-loop architecture is then designed at the gain layer, which integrates a leaky integrator with anti-windup back-calculation to mitigate integrator drift and saturation transients. Furthermore, within a Lyapunov-based analytical framework, we establish that the proposed tracking control scheme for multi-UAV systems guarantees three fundamental properties: global boundedness of all adaptive states, input-to-state stability (ISS) under deterministic disturbances, and mean-square boundedness (MSB) when subject to stochastic perturbations.

2. PROBLEM FORMULATION

2.1 The Multi-UAV Tracking Model

In this work, we consider a phase-shifted circular-reference tracking problem for N homogeneous UAVs operating in the two-dimensional x–z plane. Define first the index $\mathcal{V} = \{1, \dots, N\}$. Each UAV is modeled as a perturbed double-integrator system

$$\mathrm{d}p_i = v_i\,\mathrm{d}t, \quad \mathrm{d}v_i = \big(u_i + d_{w,i}(t)\big)\,\mathrm{d}t + G_i\,\mathrm{d}W_{t,i}, \quad i \in \mathcal{V}, \tag{1}$$

where $p_i, v_i, u_i \in \mathbb{R}^2$ denote the position vector, velocity vector, and outer-loop acceleration command of the i-th UAV; $d_{w,i}(t) \in \mathbb{R}^2$ represents a bounded deterministic disturbance, see e.g., a wind-shear model; $W_{t,i} \in \mathbb{R}^2$ is standard Brownian motion; and $G_i \in \mathbb{R}^{2\times 2}$ denotes the noise-intensity matrix. The stochastic term is understood in the Itô sense. We further consider the actuator saturation constraints in the UAV dynamics, given by

$$u_i \in \mathcal{U} := \{\, u \in \mathbb{R}^2 : \|u\|_\infty \le u_{\max} \,\}. \tag{2}$$

Specifically, the actuator saturation operator acts componentwise and satisfies a global Lipschitz condition. To define the circular-reference tracking task, let the reference center be $c \in \mathbb{R}^2$, the radius $r > 0$, and the angular velocity $\omega > 0$. Furthermore, the i-th vehicle is assigned a phase offset of $\Delta\theta_i := 2\pi(i-1)/N$, from which the reference trajectory and its derivative are given by

$$\begin{cases} p_{r,i}(t) = c + r[\cos(\omega t + \Delta\theta_i), \sin(\omega t + \Delta\theta_i)]^\top, \\ v_{r,i}(t) = \dot{p}_{r,i}(t) = r\omega[-\sin(\omega t + \Delta\theta_i), \cos(\omega t + \Delta\theta_i)]^\top, \\ a_{r,i}(t) = \dot{v}_{r,i}(t) = -r\omega^2[\cos(\omega t + \Delta\theta_i), \sin(\omega t + \Delta\theta_i)]^\top, \end{cases} \tag{3}$$

with $p_{r,i}, v_{r,i}, a_{r,i} \in \mathbb{R}^2$. To enable error-driven control, define the tracking errors for each UAV as $e_{p,i} := p_i - p_{r,i}$ and $e_{v,i} := v_i - v_{r,i}$. In accordance with Trentelman et al. (2002), we introduce two stacking rules:

$$\begin{cases} e_p := \mathrm{col}\{e_{p,1}, \dots, e_{p,N}\} \in \mathbb{R}^{N\times 2}, \\ G := \mathrm{diag}\{G_1, \dots, G_N\}. \end{cases} \tag{4}$$

Here, G is a block-diagonal noise-intensity matrix, whereas other vector-valued signals, including e_v, u, a_r, d_w, and $\mathrm{d}W_t$, are stacked by the same column rule as e_p. Before proceeding, we present three standard assumptions concerning the perturbed double-integrator dynamics.

Assumption 1: The disturbance $d_{w,i} \in \mathcal{L}_\infty$ is assumed to be piecewise continuous, while the noise-intensity matrix G_i associated with the Brownian motion is a bounded constant matrix. Hence, the bounded intermittent and piecewise-varying gusts are included.

Assumption 2: The actuator mismatch $\Delta(t)$ has bounded components, with subvector satisfying $\|\Delta_i(t)\| \le \Delta_{i,\max}$. The gains k_{aw} and k_{leak} are selected to ensure boundedness of the integral error e_i and the components of $\Delta(t)$. A conservative sufficient choice is given by

$$k_{\mathrm{leak}} \ge \frac{e_{p,i}^{\max} + k_{\mathrm{aw}}\Delta_{i,\max}}{e_i^{\max}}, \tag{5}$$

where $e_{p,i}^{\max}$ and $e_i^{\max}$ denote the prescribed bounds of the position-tracking error and integral states, respectively.

Assumption 3: The vector $\boldsymbol{\theta}_i(t) := (\alpha_i(t), \beta_i(t), \kappa_i(t))$ is well-defined for all t and satisfies $\left\|\dot{\boldsymbol{\theta}}_i(t)\right\| \le L$ for $L > 0$.

Remark 1: The circular pattern is generated by the shared reference parameters (c, r, ω) and the fixed offsets $\Delta\theta_i$, whereas each UAV relies on local tracking feedback for control. The stacked notation is introduced purely for compact analytical representation and does not imply any neighbor-coupled consensus dynamics. Furthermore, each UAV measures its own position and velocity and receives the reference parameter $(c, r, \omega, \Delta\theta_i)$ from a synchronized reference generator. Communication delays and packet losses are neglected in the present model. Moreover, the consideration in Assumption 3 follows from the saturated γ-dynamics, the bounded $\tanh(\cdot)$ mapping, first-order λ_{eff} dynamics, and the smooth gain maps.

2.2 The Dual-Loop Structure

To maintain bounded and smooth adaptive gains under strong disturbances and stochastic perturbations, we adopt a dual-loop architecture with a fast trend loop and a slow gain-tracking loop. Specifically, the fast loop extracts filtered error-trend information before gain modulation. To ensure that the resulting gains remain continuous and bounded, we define the local error energy as

$$\begin{cases} E_i(t) := \|e_{p,i}(t)\|^2 + \|e_{v,i}(t)\|^2, \\ \dot{\bar{E}}_i(t) = -\dfrac{1}{\tau}\big(\bar{E}_i(t) - E_i(t)\big), \end{cases} \tag{6}$$

for the i-th UAV, where $\bar{E}_i(t) \in \mathbb{R}$ denotes the first-order low-pass filtered signal of $E_i(t) \in \mathbb{R}$ with time constant $\tau > 0$, capturing its short-term averaged error. Similarly, we then stack the signals as $E(t) := \mathrm{col}\{E_1, E_2, \dots, E_N\} \in \mathbb{R}^{N\times 1}$, and $\bar{E}(t) := \mathrm{col}\{\bar{E}_1, \bar{E}_2, \dots, \bar{E}_N\} \in \mathbb{R}^{N\times 1}$. Furthermore, we define the error-trend function $s(t)$ as

$$s(t) = \bar{E}(t) - E(t) \in \mathbb{R}^{N\times 1}, \tag{7}$$

which quantifies whether the current error is improving or worsening compared to its recent behavior. Specifically, $E_i > \bar{E}_i$ leads to $s_i < 0$, indicating error deterioration, whereas $E_i < \bar{E}_i$ yields $s_i > 0$, indicating error recovery.

It is worth noting that although $s(t)$ captures the raw trend information, it is typically not used directly by the controller. Inspired by the annealing algorithm, we further transform $s(t)$ into a fast-loop parameter

$$\dot{\gamma}(t) = -k_g\gamma(t) + k_s\mathrm{sat}\left(\frac{s(t)}{\delta_g}\right), \tag{8}$$

wherein $k_g, k_s, \delta_g > 0$ and $|\mathrm{sat}| \leq 1$; $\gamma \in \mathbb{R}^{N\times 1}$ denotes a smooth, bounded, and Lipschitz-continuous trend integrator; the saturation function $\mathrm{sat}(\cdot)$ limits each input component to the range $[-1, 1]$ componentwise; $\delta_g > 0$ is a sensitivity scaling parameter; $k_s > 0$ characterizes the driving strength from $s(t)$ to γ; $k_g > 0$ represents the leakage-integration coefficient, which suppresses accumulation and ensures the boundedness of γ.

Between the trend integrator γ and the closed-loop gain, we introduce a slow-loop as follows,

$$\lambda^*(t) = \lambda_{\min}\mathbf{1}_{N\times 1} + (\lambda_{\max} - \lambda_{\min})\frac{\mathbf{1}_{N\times 1} + \tanh(\rho\,\gamma(t))}{2}, \tag{9}$$

$$\dot{\lambda}_{\mathrm{eff}}(t) = -\eta\big(\lambda_{\mathrm{eff}}(t) - \lambda^*(t)\big), \tag{10}$$

which provides a tunable transition mapping to track γ. Here, $\lambda^*(t)$ and $\lambda_{\mathrm{eff}}(t)$ are elements of $\mathbb{R}^{N\times 1}$, while γ_i and $\lambda_{\mathrm{eff},i}$ are the dual-loop scalars acting on the i-th UAV, respectively. The function $\tanh(\cdot)$ provides a monotonic bounded mapping from γ_i to the interval $[\lambda_{\min}, \lambda_{\max}]$. $\rho > 0$ serves as a slope-shaping factor that adjusts the sensitivity of this mapping. In particular, the slow-loop variable $\lambda_{\mathrm{eff}}(t)$ tracks $\lambda^*(t)$ through a first-order lag with rate $\eta > 0$. A larger η enables faster tracking and a more aggressive transient response, but typically at the expense of reduced robustness.

Remark 2: According to the sign convention in (7), error deterioration decreases $\lambda_{\mathrm{eff},i}$ and increases the PID gains in (13)-(14), while error recovery compresses the gains to mitigate the risk of saturation.

2.3 Annealed Gain Scheduling

From the Robbins–Monro step-size conditions from time-varying gain schemes, we recall the classical gain-scheduling

$$u_i(k) = -\alpha_k\left(\sum_{j=1}^{N} L_{ij}\,x_j(k) + g_i\big(x_i(k)\big)\right), \tag{11}$$

which must satisfy the following two constraints on the time-varying gain α_k

$$\sum_{k=0}^{\infty}\alpha_k = \infty, \quad \sum_{k=0}^{\infty}\alpha_k^2 < \infty, \tag{12}$$

where L_{ij} denotes the Laplacian matrix of the communication graph with $L\mathbf{1} = 0$, $g_i(\cdot)$ represents the local feedback, see e.g., the gradient ∇f_i or a linear state feedback Kx_i and α_k is the globally synchronized time-varying gain. It is worth emphasizing that although this model showed in (11) is not directly applicable to the highly dynamic environments considered in this paper, prior results in Li et al. (2010) indicate that, under the conditions of a connected graph, bounded disturbance moments, and appropriate monotonicity on g_i, the aforementioned control law, together with its step-size conditions, can still ensure consensus and keep noise accumulation bounded.

Motivated by this observation, our gain-function design adopts the same bounded-gain principle, while further modifying the time-varying gain into an error-driven form and incorporating an annealing mechanism to enhance adaptability in highly disturbed environments. Using the slow-loop parameter $\lambda_{\mathrm{eff}}(t)$ as a reference benchmark, the nominal gain is compressed in an annealing manner, which is explicitly given as follows

$$\alpha_i(t) = \frac{K_{p0}}{1 + \lambda_{\mathrm{eff},i}(t)^a}, \quad \beta_i(t) = \frac{K_{v0}}{1 + \lambda_{\mathrm{eff},i}(t)^a}, \tag{13}$$

with $K_{p0}, K_{v0}, a > 0$. Herein, a denotes the exponent constraint constant, and $\alpha_i(t), \beta_i(t) \in \mathbb{R}$ represent the position and velocity feedback gains for the second-order integrator model of the i-th UAV, together forming the baseline PD tracking control law. To further mitigate steady-state errors, an additional integral term is incorporated.

$$\kappa_i(t) = \frac{K_{i0}}{1 + \lambda_{\mathrm{eff},i}(t)^a}, \quad K_{i0} \geq 0, \tag{14}$$

where $\kappa_i(t) \in \mathbb{R}$ is the integral feedback gain. The resulting controller produces an augmented PID law, with initial gains denoted by K_{p0}, K_{v0}, K_{i0}. In contrast to the PD case, the closed-loop system becomes third-order, implying that its characteristic polynomial must satisfy the Hurwitz stability criterion. Consequently, the augmented dynamics need to be included in the Lyapunov state analysis. Since $\lambda_{\mathrm{eff},i}(t) \in [\lambda_{\min}, \lambda_{\max}]$ is bounded, the gains $\alpha_i(t), \beta_i(t)$, and $\kappa_i(t)$ are also bounded. For the sake of compact notation, we define $\alpha(t), \beta(t)$, and $\kappa(t)$ as the average values of the respective gains over all UAVs. For subsequent analysis, define the diagonal gain matrices as

$$\begin{aligned} P(t) &:= \mathrm{diag}\{\alpha_i(t)\}_{i=1}^N, \quad V(t) := \mathrm{diag}\{\beta_i(t)\}_{i=1}^N, \\ I_z(t) &:= \mathrm{diag}\{\kappa_i(t)\}_{i=1}^N, \qquad P, V, I_z \in \mathbb{R}^{N\times N}. \end{aligned} \tag{15}$$

We further introduce the compact gain domain

$$\Theta := [\underline{\alpha}_i, \overline{\alpha}_i] \times [\underline{\beta}_i, \overline{\beta}_i] \times [\underline{\kappa}_i, \overline{\kappa}_i]. \tag{16}$$

and treat $\theta_i(t) := (\alpha_i(t), \beta_i(t), \kappa_i(t))$ as a time-varying, measurable parameter vector, which always satisfies $\theta_i(t) \in \Theta$. Under the fast-slow time-scale separation, there always exists a constant $L > 0$ such that $\|\dot{\theta}_i(t)\| \leq L$ for all t, i.e., the variation rates of the PID gains $\alpha_i(t), \beta_i(t)$, and $\kappa_i(t)$ are uniformly bounded, thereby ensuring that the closed-loop vector field remains continuous and bounded. More specifically, the boundedness of $\dot{\theta}_i(t)$ is ensured by the bounded γ- and λ_{eff}-dynamics, together with the smooth gain mappings in (13)–(14).

Within the augmented PID control law, however, the additional integral term may lead to integrator drift when the actuators are saturated. To address this, we incorporate a leaky integration strategy and anti-windup compensation into the original PID control law. Retaining the scaling matrix specified in (15), the integral term is designed as

$$\begin{cases} u_{\mathrm{unsat}} = -P(t)e_p - V(t)e_v - I_z(t)e_i, \\ \dot{e}_i = e_p - k_{\mathrm{leak}}e_i + k_{\mathrm{aw}}(u_{\mathrm{sat}} - u_{\mathrm{unsat}}), \\ u_{\mathrm{sat}} = \mathrm{sat}(u_{\mathrm{unsat}}, u_{\max}), \end{cases} \tag{17}$$

where $k_{\mathrm{leak}} > 0$ and $k_{\mathrm{aw}} > 0$ denote the leaky integration and anti-windup feedback coefficients, respectively; $u_{\mathrm{unsat}} \in \mathbb{R}^{N\times 2}$ represents the unsaturated control input; $u_{\mathrm{sat}} \in \mathbb{R}^{N\times 2}$ is the output of the saturation function $\mathrm{sat}(\cdot)$, which constrains each element of the output command vector to $[-u_{\max}, u_{\max}]$. In case of saturation, the correspond-

ing error is fed back into the integrator, thereby curbing windup. Here, the anti-windup mechanism prevents accumulation induced by saturation, while the leakage term ensures continuous dissipation of the integral state in the presence of residual errors and stochastic fluctuations. Specifically, the actuator mismatch parameter is given by

$$\Delta(t) := u_{\text{sat}} - u_{\text{unsat}}, \tag{18}$$

with $\Delta(t) \in \mathbb{R}^{N\times 2}$, whose components satisfy $|\Delta_i(t)| \le \Delta_{i,\max}$ for all $i \in \mathcal{V}$. Using the stacked notation and gain matrices above, the tracking-error subsystem with leaky anti-windup compensation is given by

$$\begin{cases} \mathrm{d}e_p = e_v\,\mathrm{d}t, \\ \mathrm{d}e_v = (-Pe_p - Ve_v - I_z e_i + d_w + \Delta)\,\mathrm{d}t \\ \qquad\quad + G\,\mathrm{d}W_t, \\ \mathrm{d}e_i = (e_p - k_{\text{leak}} e_i + k_{\text{aw}}\Delta)\,\mathrm{d}t. \end{cases} \tag{19}$$

Together with (6), (8), and (10), (19) forms the complete closed-loop system.

For the LMI analysis, the two Cartesian coordinates are treated in the same way. For either coordinate, let $e_P, e_V, e_I \in \mathbb{R}^{N\times 1}$ collect the corresponding scalar components of e_p, e_v, e_i, respectively. The Lyapunov state vector is then $\Xi := \mathrm{col}\{e_P, e_V, e_I, \bar{E}, \gamma, \lambda_{\text{eff}}\} \in \mathbb{R}^{6N\times 1}$. For notational simplicity, the coordinate superscript is omitted; the same argument applies to the other coordinate.

3. MAIN RESULTS

Our main results are presented in this section. First, we derive verifiable vertex-based linear matrix inequality (LMI) conditions over a convex polytope and establish the ISS property of the proposed tracking scheme in the presence of bounded deterministic disturbances. By leveraging these results, we then demonstrate that the closed-loop system achieves MSB under stochastic disturbances.

3.1 ISS amid Deterministic Disturbances

We begin by examining the deterministic component of the multi-UAV tracking system, constructing its polytopic representation, and subsequently analyzing the ISS property of the closed-loop system under bounded inputs. Denote

$$\mathbf{z} \triangleq \left[e_P^\top e_V^\top e_I^\top\right]^\top \in \mathbb{R}^{3N\times 1}. \tag{20}$$

Using the bounded-gain construction above, the time-varying gains can be written in a scaling-matrix form. The stacked dynamics then become

$$\dot{\mathbf{z}} = A(P, V, I_z)\,\mathbf{z}, \tag{21}$$

with

$$A(P, V, I_z) = \begin{bmatrix} 0 & I_N & 0 \\ -P & -V & -I_z \\ I_N & 0 & -k_{\text{leak}} I_N \end{bmatrix}. \tag{22}$$

Based on the gain construction in Section II, the gains $(\alpha_i, \beta_i, \kappa_i)$ are bounded. Consequently, the affine family $A(P, V, I_z)$ is enclosed by the convex hull of eight extreme matrices, with the vertex set defined as $\mathcal{V} := \{(P, V, I_z) \mid P \in \{\alpha_{\min} I_N, \alpha_{\max} I_N\},\ V \in \{\beta_{\min} I_N, \beta_{\max} I_N\},\ I_z \in \{k_{\min} I_N, k_{\max} I_N\}\}$. The associated common quadratic certificate is the existence of $D = D^\top \succ 0$ and $W = W^\top \succ 0$ such that

$$A_\nu^\top D + D A_\nu \preceq -W, \quad \nu = 1, \dots, 8, \tag{23}$$

for all vertex matrices A_ν generated by $\mathcal{V}$.

Remark 3: If there exist matrices $D \succ 0$ and $W \succ 0$ satisfying the vertex-LMI condition (23), then for all admissible $(\alpha, \beta, \kappa_i)$, the third-order tracking-error subsystem is uniformly quadratically stable under a common quadratic Lyapunov function. In the absence of disturbances where $d_w \equiv 0$, $\Delta \equiv 0$, and $G \equiv 0$, by choosing $V(\mathbf{z}) = \mathbf{z}^\top D \mathbf{z}$, one obtains $\dot{V} \le -\lambda_{\min}(W)\|\mathbf{z}\|^2$. Thus, the tracking error $\mathbf{z}(t)$ converges exponentially to zero.

Remark 4: The dual-loop states γ and λ_{eff} serve only to schedule the admissible gains (P, V, I_z) via (13) and (14), thereby preserving the polytopic structure.

To quantify the system's stability, we employ the negative-feedback realization presented in (19) to formulate a composite Lyapunov candidate

$$V(\Xi) = \mathbf{z}^\top D \mathbf{z} + \tfrac{1}{2}\,\gamma^\top C_\gamma\,\gamma + \tfrac{1}{2}\,\mu^\top C_\lambda\,\mu \in \mathbb{R}, \tag{24}$$

with $\mathbf{z}$ given by (20), $D = D^\top \succ 0$, $C_\gamma = C_\gamma^\top \succ 0$, $C_\lambda = C_\lambda^\top \succ 0$, $D \in \mathbb{R}^{3N\times 3N}$, and $C_\gamma, C_\lambda \in \mathbb{R}^{N\times N}$. Define the mismatch variable $\mu := \lambda_{\text{eff}} - \lambda^*(\gamma) \in \mathbb{R}^{N\times 1}$. For brevity, we combine the bounded deterministic disturbance and the deviation induced by actuator saturation as

$$\tilde{d}(t) \doteq \left[\mathbf{0}_N^\top (d_w(t) + \Delta(t))^\top \mathbf{0}_N^\top\right]^\top \in \mathbb{R}^{3N\times 1}. \tag{25}$$

Theorem 1: Given that *Assumptions 1–3* hold, the vertex-LMI condition (23) is feasible, and $\tilde{d} \in L_\infty$, the closed-loop system (19) achieves ISS with respect to $\tilde{d}(t)$, implying that there exist a class-$\mathcal{KL}$ function β_d and a class-$\mathcal{K}$ function γ_d such that

$$\begin{aligned} \big\|\,(e_p(t), e_v(t), e_i(t))\,\big\| \le \beta_d\big(\,\big\|\,(e_p(0), e_v(0), e_i(0))\,\big\|,\, t\big) \\ + \gamma_d\Big(\sup_{0\le\tau\le t} \|\tilde{d}(\tau)\|\Big). \end{aligned} \tag{26}$$

Proof: From the deterministic component of (19) together with the structure in (22), we have

$$\dot{\mathbf{z}} = A(P, V, I_z)\,\mathbf{z} + B\,\tilde{d}(t), \tag{27}$$

where $B \in \mathbb{R}^{3N\times 3N}$ is a constant input matrix. Taking the derivative of V along the trajectories and applying the vertex–LMI condition $A^\top D + DA \preceq -W$, we obtain $\dot{V} = \mathbf{z}^\top (A^\top D + DA)\mathbf{z} + 2\,\mathbf{z}^\top DB\,\tilde{d} + \gamma^\top C_\gamma\,\dot{\gamma} + \mu^\top C_\lambda\,\dot{\mu}$. Using the boundedness and dissipativity of the trend and gain-tracking channels, there exist $Q_\gamma, Q_\lambda \succeq 0$ such that

$$\begin{cases} \gamma^\top C_\gamma \dot{\gamma} \le -\,\gamma^\top Q_\gamma \gamma, \\ \mu^\top C_\lambda \dot{\mu} \le -\,\mu^\top Q_\lambda \mu. \end{cases} \tag{28}$$

Therefore, we obtain

$$\dot{V} \le -\,\mathbf{z}^\top W \mathbf{z} + 2\mathbf{z}^\top DB\tilde{d} - \gamma^\top Q_\gamma \gamma - \mu^\top Q_\lambda \mu. \tag{29}$$

For identical UAVs, one may set $C_\gamma = c_\gamma I_N$ and $C_\lambda = c_\lambda I_N$, so that the corresponding dissipative terms reduce to scalar-weighted quadratic terms. The remainder of the proof is unchanged. Applying *Young's inequality* to the cross term $2\mathbf{z}^\top DB\tilde{d}$, for any $\varepsilon > 0$, gives

$$2\mathbf{z}^\top DB\tilde{d} \le \varepsilon\,\|\mathbf{z}\|^2 + \varepsilon^{-1}\,\|DB\|^2\,\|\tilde{d}\|^2. \tag{30}$$

Choose $\varepsilon = \frac{1}{2}\,\lambda_{\min}(W)$, and note that

$$\begin{cases} \lambda_{\min}(D)\,\|\mathbf{z}\|^2 \le \mathbf{z}^\top D \mathbf{z} \le \lambda_{\max}(D)\,\|\mathbf{z}\|^2, \\ \lambda_{\min}(W)\,\|\mathbf{z}\|^2 \le \mathbf{z}^\top W \mathbf{z}, \\ \qquad \gamma^\top Q_\gamma \gamma \ge \lambda_{\min}(Q_\gamma)\,\|\gamma\|^2, \\ \qquad \mu^\top Q_\lambda \mu \ge \lambda_{\min}(Q_\lambda)\,\|\mu\|^2. \end{cases} \tag{31}$$

Thus, there exist constants $c_1, c_2, c_3, c_4 > 0$ such that

$$\dot{V} \le -c_1\|\mathbf{z}\|^2 - c_2\|\gamma\|^2 - c_3\|\mu\|^2 + c_4\|\tilde{d}\|^2. \tag{32}$$

By positive definiteness property, it follows that

$$\underline{c}\big(\|\mathbf{z}\|^2 + \|\gamma\|^2 + \|\mu\|^2\big) \le V \le \bar{c}\big(\|\mathbf{z}\|^2 + \|\gamma\|^2 + \|\mu\|^2\big),$$

where $\underline{c} = \min\{\lambda_{\min}(D),\ \frac{1}{2}\lambda_{\min}(C_\gamma),\ \frac{1}{2}\lambda_{\min}(C_\lambda)\} > 0$ and $\bar{c} = \max\{\lambda_{\max}(D),\ \frac{1}{2}\lambda_{\max}(C_\gamma),\ \frac{1}{2}\lambda_{\max}(C_\lambda)\} > 0$. As a consequence, there exists $c_5 > 0$ such that

$$\dot{V} \le -c_5 V + c_4\,\|\tilde{d}\|^2. \tag{33}$$

Solving the scalar differential inequality in (33) yields

$$V(t) \le e^{-c_5 t}V(0) + \frac{c_4}{c_5}\sup_{0\le\tau\le t}\|\tilde{d}(\tau)\|^2. \tag{34}$$

By the norm equivalence between V and $\|\mathbf{z}\|^2 + \|\gamma\|^2 + \|\mu\|^2$, and taking the square root of both sides, we obtain $\mathcal{KL}$- and $\mathcal{K}$-functions

$$\beta_d(r,t) = \sqrt{\frac{\bar{c}}{\underline{c}}}e^{-\frac{c_5}{2}t}\,r, \gamma_d(s) = \sqrt{\frac{c_4}{c_5\,\underline{c}}}s, \tag{35}$$

where $r = \|(e_p(0), e_v(0), e_i(0))\|$. Thus, the bound in (26) is established, demonstrating the boundedness of the tracking errors under deterministic disturbances. ■

Corollary 1: Consider the multi-UAV tracking dynamics described by (19). The following statements hold.

(i) If $\tilde{d} \equiv 0$, then $\dot{V} \le -c_5 V$ and $V(t)$ decays exponentially.

(ii) If $d_w \equiv 0$ and $\Delta \equiv 0$, then each component of the error triple (e_p, e_v, e_i) converges to zero exponentially.

3.2 MSB under Stochastic Perturbations

In this section, we consider a more general setting where the input channels are subject to stochastic disturbances, with the aim of analyzing the closed-loop tracking-error stability. Specifically, the stochastic perturbations are modeled as Brownian noise. Under *Assumptions 1–3*, the dynamics in (19) can be rewritten in the following Itô form

$$\begin{cases} \mathrm{d}e_p = e_v\,\mathrm{d}t, \\ \mathrm{d}e_v = \big(-Pe_p - Ve_v - I_z e_i + d_w + \Delta\big)\,\mathrm{d}t + G\,\mathrm{d}W_t, \\ \mathrm{d}e_i = \big(e_p - k_{\text{leak}}e_i + k_{\text{aw}}\Delta(t)\big)\,\mathrm{d}t. \end{cases} \tag{36}$$

Theorem 2: Given that the vertex-LMI condition (23) holds and the disturbances satisfy *Assumptions 1–2*, then there exist positive constants c_m, c_d, c_G for which the Lyapunov candidate $V(\Xi)$ satisfies

$$\frac{\mathrm{d}}{\mathrm{d}t}\,\mathbb{E}\big[V\big(\Xi(t)\big)\big] \le -c_m\mathbb{E}\|\mathbf{z}(t)\|^2 + c_d\|\tilde{d}\|_\infty^2 + c_G\,\|G\|_F^2. \tag{37}$$

Moreover, there exist constants $c_{\text{sup}}, c_{\text{add}} > 0$ such that

$$\sup_{t\ge0}\,\mathbb{E}\|\mathbf{z}(t)\|^2 \le c_{\text{sup}}\,\mathbb{E}\|\mathbf{z}(0)\|^2 + \frac{c_{\text{sup}}}{c_m}\Big(c_d\,\|\tilde{d}\|_\infty^2 + c_G\,\|G\|_F^2\Big) + c_{\text{add}}. \tag{38}$$

The proof follows from Itô's formula and the standard quadratic Lyapunov argument established in Theorem 1. The detailed proof is omitted here due to space limitations.

Corollary 2: Building on Theorem 2, some results follow.

(i) There exists $R > 0$ such that $\limsup_{t\to\infty}\mathbb{E}\|\mathbf{z}(t)\|^2 \le R$. Then, for any $\varepsilon > 0$ and any fixed $t \ge T$, Chebyshev's inequality yields $\mathbb{P}\{\|\mathbf{z}(t)\| \ge \varepsilon\} \le \frac{1}{\varepsilon^2}\mathbb{E}\|\mathbf{z}(t)\|^2 \le \frac{R}{\varepsilon^2}$.

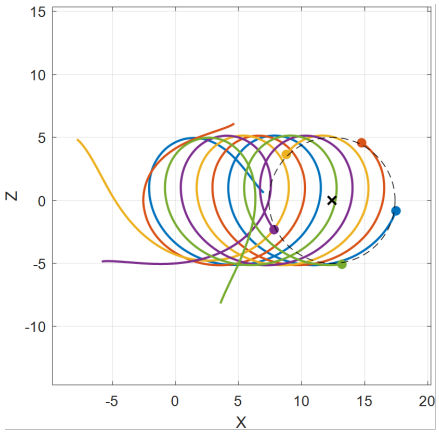


Fig. 1. Tracking trajectories of the multi-UAV system.

(ii) Let $\varepsilon = \sqrt{R/\varsigma}$. Then $\Pr\{\|\mathbf{z}(t)\| \le \sqrt{R/\varsigma}\} \ge 1 - \varsigma$. Moreover, $R = O(\|\tilde{d}\|_\infty^2 + \|G\|_F^2)$. Hence, the closed-loop system is ultimately mean-square bounded.

Remark 5: When $G = 0$, the MSB property reduces to deterministic ISS. Under the additional condition of $d_w \equiv 0$ and $\Delta \equiv 0$, the common quadratic Lyapunov function further shows uniform exponential stability of the tracking-error origin.

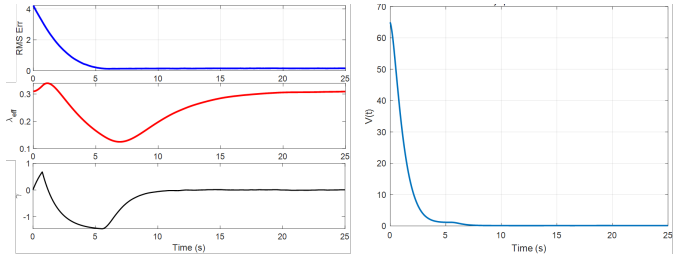
4. NUMERICAL EXAMPLES

This section evaluates the proposed dual-loop annealed PID controller in a phase-shifted circular-reference tracking task with $N = 5$ UAVs. The reference parameters are $r = 5\,\text{m}$ and $\omega = 0.5\,\text{rad/s}$, and the trend filter uses $\omega_e = 2.0\,\text{s}^{-1}$, i.e., $\tau = 1/\omega_e = 0.5\,\text{s}$, with $dt = 0.01\,\text{s}$. The initial phases are uniformly distributed on the ring with small random perturbations. The dual-loop parameters are set as $k_g = 0.8$, $k_s = 1.2$, $\delta_g = 0.05$, $\rho = 1.0$, $\eta = 0.3$, $\lambda_{\min} = 0.02$, and $\lambda_{\max} = 0.6$, while the PID baselines are $K_{p0} = 10$, $K_{v0} = 8$, $K_{i0} = 2.5$, and $a = 0.9$. Deterministic disturbances are generated by a stationary 2-D AR(2) wind-shear model $w_k = a_1 w_{k-1} + a_2 w_{k-2} + \sigma\varepsilon_k$, with $a_1 = 0.7$, $a_2 = 0.2$, and $\sigma = 0.05$. Brownian perturbations with $\sigma_b = 0.02$ are added through the Euler–Maruyama term $\sigma_b\sqrt{dt}\,\xi_k$, where $\xi_k \sim \mathcal{N}(0, I)$.

The main numerical results are shown in Figs. 1–3. Fig. 1 shows that the proposed controller accurately tracks the phase-shifted circular references under deterministic and stochastic perturbations. As shown in Fig. 2, the RMS tracking error and Lyapunov candidate $V(t)$ decay rapidly, while γ and λ_{eff} evolve smoothly within their bounds, indicating the expected annealed adaptation and time-scale separation. Fig. 3 further shows the actuator and Lyapunov-evidence responses. The initially near-saturated inputs are quickly desaturated by the anti-windup back-calculation and gain compression, and only small steady-state oscillations remain. The near-zero least-squares slope in Fig. 3(b) is empirically consistent with the derived ISS/MSB-type dissipation inequality.

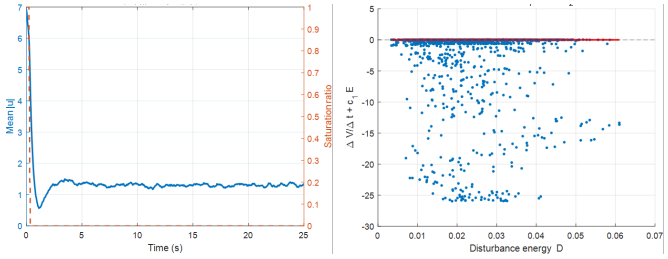
5. CONCLUSIONS

This paper has addressed the stability of phase-shifted circular-reference tracking for multi-UAV systems under



(a) (b)

Fig. 2. Adaptive parameter and Lyapunov function evolution: (a) dual-loop parameters and RMS error; (b) Lyapunov function evolution.



(a) (b)

Fig. 3. Actuator saturation and Lyapunov evidence: (a) actuator saturation; (b) Lyapunov evidence scatter.

simultaneous deterministic and stochastic disturbances, as well as actuator saturation. A trend-driven dual-loop PID tracking controller with annealed adaptive gains was proposed, whereby the verifiable ISS and MSB guarantees were established within a vertex-LMI framework. Numerical examples confirm rapid convergence of tracking errors and Lyapunov energy, swift actuator desaturation, and low steady-state control effort. Moreover, the proposed method achieves robust performance with a compact set of tuning parameters via annealed adaptation, thereby ensuring control continuity and low computational cost.

REFERENCES

Y.-H. Su, P. Bhowmick, and A. Lanzon. A robust adaptive formation control methodology for networked multi-UAV systems with applications to cooperative payload transportation. *Control Engineering Practice*, 138: 105608, 2023.

K. Wang, Q. Ma, C. Shen, and J. Lu. Application of uncertainty to out-of-distribution detection for autonomous driving perception safety. *IEEE Transactions on Intelligent Transportation Systems*, 26(8):11276–11293, 2025.

J. Sun, Y. Meng, J. Huang, et al. Distributed cooperative control with collision avoidance for spacecraft swarm reconfiguration via reinforcement learning. *Acta Astronautica*, 205:95–109, 2023.

Z. Pan, C. Zhang, Y. Xia, H. Xiong, and X. Shao. An improved artificial potential field method for path planning and formation control of the multi-UAV systems. *IEEE Transactions on Circuits and Systems II: Express Briefs*, 69(3):1129–1133, 2022.

Q. Wei, X. Wang, X. Zhong, et al. Consensus control of leader–following multi-agent systems in directed topology with heterogeneous disturbances. *IEEE/CAA Journal of Automatica Sinica*, 8(2):423–431, 2021.

G. De Pasquale, B. Fidan, M.E. Valcher, et al. Consensus for clusters of agents with cooperative and antagonistic relationships. *Automatica*, 135:110002, 2022.

S. Guo and X. Meng. Fully distributed control of multiagent networks with edge-based event-triggered communication. *IEEE Transactions on Automatic Control*, 68(9):5630–5637, 2023.

J. Li, X. Wang, et al. High-performance control method for six-degree-of-freedom micro-motion stage based on high-order sliding mode control theory. *IEEE Transactions on Power Electronics*, 39(8):1–14, 2024.

A. Hakobyan and I. Yang. Wasserstein distributionally robust control of partially observable linear stochastic systems. *IEEE Transactions on Automatic Control*, 69(9):6121–6136, 2024.

G. Tao. Adaptive output tracking control with reference model system uncertainties. *Automatica*, 174:112174, 2025.

H. Ahmadian, M.M. Arefi, A. Khayatian, et al. An improved L_1 adaptive high-gain observer with guaranteed performance and stability robustness for uncertain Euler–Lagrange systems. *Ocean Engineering*, 311: 118684, 2024.

Y. Sun, H. Deng, et al. Event-triggered control of Itô stochastic nonlinear delayed systems with state quantization. *International Journal of Robust and Nonlinear Control*, 34(5):3167–3188, 2024.

Q. Mao, Y. Xu, J. Chen, J. Chen, and T. T. Georgiou. Maximization of gain/phase margins by PID control. *IEEE Transactions on Automatic Control*, 70(1):34–49, 2025.

Q. Mao, Y. Xu, J. Chen, and T. T. Georgiou. Implementation-oriented filtered PID control: Optimization of robustness margins. *Automatica*, 152: 110974, 2023.

A. Barzegar, F. Hamze, C. Amey, and J. Machta. Optimal schedules for annealing algorithms. *Physical Review E*, 109(6):065301, 2024.

H.L. Trentelman, J.C. Willems, et al. Synthesis of dissipative systems using quadratic differential forms: Part I. *IEEE Transactions on Automatic Control*, 47(1):53–69, 2002.

T. Li, L. Xie, et al. Consensus conditions of multi-agent systems with time-varying topologies and stochastic communication noises. *IEEE Transactions on Automatic Control*, 55(9):2043–2057, 2010.